Supplementary Material for "Optimal Electric Ship-to-Grid Dispatch Considering Electrochemical-Thermal-Coupled Battery Cell Constraints of Thermal and Voltage Limits"

Chao Lei, *Member, IEEE*, and Y. Christine Chen, *Member, IEEE*

I. Derivations of (4a)

Substitute (1) into (2) and rearrange the resultant to yield

$$\widehat{T}_{i,j+1}^{t} = \Big(1 - \frac{h_{c,i}A_{s,i}\Delta h}{m_i C_{p,i}}\Big)T_{i,j}^{t} + \frac{\Delta h}{m_i C_{p,i}}(\epsilon H_{e,i}^{t+\Delta t} + h_{c,i}A_{s,i}T_{\text{amb}}), \tag{I-1}$$

where the variation of time-varying $H_{e,i}^{t}$ between time t and $t+\Delta t$ can be approximated by $\epsilon H_{e,i}^{t+\Delta t}$ with the constant coefficient ϵ set to 0.78. Further, substitute (1) into the corrector step in (3) to get

$$T_{i,j+1}^{t} = T_{i,j}^{t} + \frac{\Delta h}{2m_i C_{p,i}}(2\epsilon H_{e,i}^{t+\Delta t} + h_{c,i}A_{s,i}(2T_{\text{amb}} - T_{i,j}^{t} - \widehat{T}_{i,j+1}^{t})), \tag{I-2}$$

Next, substitute (I-1) into (I-2) to get

$$T_{i,j+1}^{t} = \omega_1 T_{i,j}^{t} + \omega_2 H_{e,i}^{t+\Delta t} + \omega_3, \quad j = 0,1,2,...,n-1, \tag{I-3}$$

with ω_1, ω_2, and ω_3 as expressed in (4b)–(4d), respectively. The recurrence relation in (I-3) can be evaluated in closed form as

$$T_{i}^{t+\Delta t} = \omega_1^{n} T_{i}^{t} + \frac{1-\omega_1^{n-1}}{1-\omega_1}(\omega_2 H_{e,i}^{t+\Delta t} + \omega_3), \tag{I-4}$$

with boundary conditions $T_i^t = T_{i,0}^t$ and $T_i^{t+\Delta t} = T_{i,n}^t$.

II. Error Discussion for Thermal Constraints

The cell temperature error comes from the approximation of of $H_{e,i}^{t}$ in (2a). We plot the cell temperatures $T_i^{t+\Delta t}$ with respect to S_i^t and $p_{c,i}^t$ or $p_{d,i}^t$ from the PDE solver and our proposed discretized temperature equation (2a), where the cell temperature in the end of time period t is $T_i^t = 27$°C over $\Delta t = 15$min in Fig.1(a) and (b). In Fig.1(a), the approximate cell temperature $T_i^{t+\Delta t}$ is active on the grey plane when $(S_i^t, p_{c,i}^t)$ is below the cut lines AB and CD, otherwise it is on the light red plane. For Fig.1(b), the approximate cell temperature $T_i^{t+\Delta t}$ is the intersection of two planes. It is clear that the approximate cell temperatures $T_i^{t+\Delta t}$ by (2a) is very close to the cell temperature surface by the PDE solver in two sub-figures. The maximum errors between cell temperatures by the PDE solver and the approximate temperatures in charging and discharging modes are less than 1.2°C and 1.8°C, which can be acceptable for the S2G dispatch problem.

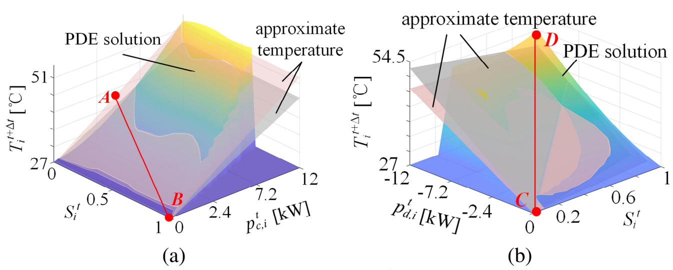

Fig. 1. Estimation of cell temperature T_i^{t+1}: (a) charge; (b) discharge.

III. Parameters for Heat Estimation and Electrochemical Kinetics

In this study, the BESS in ES_i consists of $N_i = 41$ LiFePO_4 battery modules arranged in series configuration, each with a capacity of 306.4 kWh. We select each battery cell capacity $I_{b,i} = 314$ Ah, nominal voltage $v_{\text{flat},i} = 3.4$ V with the operating voltage ranging from 2.5 V to 3.65 V, and current rate $C_{r,i}^t \in [0, \overline{C}_{r,i}]$ and $\overline{C}_{r,i} = 1.5$. For a battery cell, $\overline{p}_i \approx 3.65 \cdot 0.314 \cdot 1.5 \approx 1.7$ kW and $\overline{v} = 3.65$ V for a battery cell. Regarding thermal parameters, each battery cell has mass $m_i = 5.529$ kg and heat capacity $C_{p,i} = 1417.2$ J/(kg · K). The forced convection air cooling with four fans is available from four side openings of a battery cell with surface area $A_{s,i} = 0.1271\,\text{m}^2$, and the heat transfer coefficient is $h_{c,i} = 5.0\,\text{W}/(\text{m}^2 \cdot \text{K})$. Other parameters for electrochemical kinetics are given in Tab.I (See next page).

TABLE I
PARAMETERS FOR ELECTROCHEMICAL KINETICS

Parameter	Negative electrode	Separator	Positive electrode
electrode plate area (m^2)	0.163	0.163	0.163
electrode thickness (m)	$78 \cdot 10^{-6}$	$20 \cdot 10^{-6}$	$45 \cdot 10^{-6}$
Li^+ diffusion coefficient (m^2/s)	$3.9 \cdot 10^{-5}$	-	$1.8 \cdot 10^{-8}$
active electrode volume fraction (%)	0.6	-	0.6
electrolyte phase volume fraction (%)	0.3	-	0.3
max solid phase concentration (mol/m^3)	31507	-	49000
particle radius (m)	$6 \cdot 10^{-6}$	-	$5 \cdot 10^{-6}$
reaction rate efficiency (A/m^2)	$9.77 \cdot 10^{-2}$	-	$1.19 \cdot 10^{-2}$
exchange current density of side reaction (A/m^2)	10	-	10
initial electrolyte concentration (mol/m^3)	$1.25 \cdot 10^4$	$1.25 \cdot 10^4$	$1.25 \cdot 10^4$
Binder volume fraction(%)	0.1	-	0.1
Separator volume fraction(%)	-	0.4	-